UAV Path Planning for Maximum-Information Sensing in Spatiotemporal Data Acquisition

By:

Andreas Nordby Vibeto

andreanv@stud.ntnu.no

Supervisor: **Tor Arne Johansen**

Co-supervisor: Joo F. Fortuna

NTNU

April, 2017

Contents

Chapter 1

Introduction

Unmanned Aerial Vehcles (UAV) are today widely used in ground observation, and by equipping them with different sensors they can be used in different situations. While the use of UAV eases many cases of ground obsercation, there are some difficulties related to the attitude of the aircraft. When the sensor is attached directly to the aircraft the sensor will be coupled with the UAVs states, so that any change in the UAV states will cause a change in what is actually observed by the sensor.

A common solution to decouple the sensor from the UAV states is to attach the sensor to a gimbal which will countaract most of the movements of the UAV. While this is a good solution for decoupling, it raises some new issues regarding its weight and size. As one of the benefits of UAVs is their small size the gimbal can quickly be too big and heavy for the UAV, and it may give less effective aerodynamics. This may again lead to increased fuel consumption for the UAV.

This paper will investigate methods to reduce image errors caused by the UAVs attitude, while also avoiding the extra costs associated with a gimbal. This will be accomplished by optimizing a pre-defined curved path that is to be observed with a model of the UAV. The control method will be developed with a hyperspectral pushbroom camera that is fixed to the UAV in mind.

INSERT FIGURE THAT SHOWS UAV IN TURN AND BOTH OBSERVATION PATH AND CAMERA FOOTPRINT

1.1 Related Work

The most common method to decouple the UAV attitude states from the sensor today is to equip the aircraft with a gimbal, which allows ”NORMAL” UAV operation without losing track of the features that is to be observed. However, gimbals have limited range and if the UAV angles are to big, the features may be lost from the sensor field of view

(FOV). One solution to this problem is to use optimization [1]. Another solution that uses optimization without the use of gimbal is to put constraints on the the UAVs roll angle and altitude [2].

A simpler solution to avoid lateral movements of the FOV is to change the UAV course wby using the rudder instead of the ailerons. The rudder deflection creates a yawing moment [3] which causes the aircraft to change course. This type of controller is referred to both as a Rudder Augmented Trajectory Correction (RATC) controller [3] and a skid-to-turn (STT) controller [4]. Results show that the performance of these controllers are comparable to conventional controllers using roll to change course, and that errors in the images is greatly reduced [3] [4] [5].

While the controllers offer a solution to the control problem that reduces the errors in the images, they do not ensure that the ground path that is to be observed will always stay inside the sensors FOV. Optimization is a commonly used method for ensuring that the application succeeds at some ”outside” goal, and can be used to e.g. minimize the risk of being identified by radars [6] or plan a path that ensures that a slung load attached to a helicopter do not collide with obstacles [7]. The use of optimization to minimize the error of the sensor footprint for a fixed camera has been done by Jackson [8], by using on-board motion planning.

Jackson presents a path planner that aims to minimize the error between the target on the ground, and the footprint of a camera fixed to a UAV. To achieve this a Nonlinear Model Predictive Controller (NMPC) based on a kinodynamic (an explenation of this would be nice) model of the aircraft is created. The NMPC is compared to a PID and a sliding-mode controller that seek to follow the same path. Simulations of the three controllers show that while the PID controller had much bigger crosstrack errors than the other two, the NMPC and the sliding-mode controller had similar performance. However, the simulations proved that the NMPC controller was able to find a near optimal solution with the performance characteristics of a real-time application.

1.2 Hyperspectral Imaging

The control method developed in this paper will be developed with the use of a fixed hyperspectral, pushbroom sensor in mind. A hyperspectral sensor/camera makes it possible to accurately detect types of material from the UAV by sensing the wavelength of the received light.

1.2.1 Description

Hyperspectral imaging uses basics from spectroscopy to create images, which means that the basis for the images is the emitted or reflected light from materials [9]. The amount of light that is reflected by a material at different wavelengths is determined by several factors, and this makes it possible to distinguish different materials from each other. The reflected light is passed through a grate or a prism that splits the light into different wavelength bands, so that it can be measured by a spectrometer.

When using a hyperspectral camera for ground observation from a UAV, it is very likely that one pixel of the camera covers more than one type of material on the ground. This means that the observed wavelengths will be influenced by more than one type of material. This is called a composite or mixed spectrum [9], and the spectra of the different materials are combined additively. The combined spectra can be split into the different spectra that it is build up of by noise removal and other statistical methods which will not be covered here.

1.2.2 UAV Ground Observation

Hyperspectral imaging is already being used for ground observation from UAVs. Its ability to distinguish materials based on spectral properties means that it can be used to retrieve information that normal cameras are not able to. For example in agriculture it can be used to map damage to trees caused by bark beetles [10], or it can be used to measure environmental properties, for example chlorophyl fluorescense, on leaf-level in a citrus orchard [11].

Systems for ground observation with hyperspectral cameras can be very complex, which often leads to heavy systems. In [12], a lightweight hyperspectral mapping system was created for the use with octocopters. The purpose of the system is to map agricultural areas using a spectrometer and a photogrammetric camera, and the final ”ready-to-fly” weight of the system is 2.0 kg. The resolution of the final images made it possible to gather information on a single-plant basis, and the georeferencing accuracy was off by only a few pixels.

The tests were performed at a low altitude, maximum 120 m. While this was mainly because of local regulations, it also gave a benefit as there was less atmosphere disturbance in the measurements. The UAVs orientation data combined with surface models was used when recovering the positional data in the images. However, they found that externally produced surface models was not accurate enough as they do not take vegetation into consideration. For this reason they supplemented the existing surface models with information gathered during flight.

Chapter 2

Theory

In this chapter equations and concepts used in the assignment will be presented. In section 2.1 the relevant states of the UAV and the equations needed for calculating the camera position will be shown, and in section 2.2 the MPC method and equations will be presented.

2.1 Kinematics

What is captured by the camera, the camera footprint, when the camera is fixed to the aircraft body is dependent of the position and the attitude angles of the aircraft. In this section a model for calculating the camera footprint on the ground assuming flat earth will be presented, as well as the necessary UAV states for this thesis.

2.1.1 UAV States

The position of the UAV will be given using the North East Down (NED) coordinate frame, denoted $\{n\}$:

$$\mathbf{p}^n_{b/n} = \begin{bmatrix} N \\ E \\ D \end{bmatrix} = \begin{bmatrix} x_n \\ y_n \\ z_n \end{bmatrix}, \tag{2.1}$$

with the corresponding velocities

$$\mathbf{V}^b_g = \begin{bmatrix} u \\ v \\ w \end{bmatrix}. \tag{2.2}$$

The attitude of the UAV will be given as Euler-angles:

$$\mathbf{\Theta}_{nb} = \begin{bmatrix} \phi \\ \theta \\ \psi \end{bmatrix} \tag{2.3}$$

with corresponding angular velocities:

$$\dot{\mathbf{\Theta}}_{nb} = \begin{bmatrix} p \\ q \\ r \end{bmatrix}. \tag{2.4}$$

2.1.2 Wind and Airspeed

Wind will be introduced to the vehicle in order to test how the system withstands disturbances. Since the camera footprint is dependent only on the attitude angles of the aircraft and not the course of the aircraft, the wind will only affect the navigation of the UAV. Wind speed is given in the $\{n\}$ frame as [13]

$$\mathbf{V}_w^n = \begin{bmatrix} w_n \\ w_e \\ w_d \end{bmatrix}, \tag{2.5}$$

and the air speed $\mathbf{V}_a$ of the aircraft is given by the wind speed $\mathbf{V}_w$ and ground speed $\mathbf{V}_g$ as

$$\begin{aligned} \mathbf{V}_a &= \mathbf{V}_g - \mathbf{V}_w \\ \begin{bmatrix} u_r \\ v_r \\ w_r \end{bmatrix} &= \begin{bmatrix} u \\ v \\ w \end{bmatrix} - \mathbf{R}_n^b \begin{bmatrix} w_n \\ w_e \\ w_d \end{bmatrix} \end{aligned} \tag{2.6}$$

where $\mathbf{R}_n^b$ is the rotation matrix between the NED frame $\{n\}$ and the body frame $\{b\}$.

When in the presence of wind, the heading of the UAV isn't necessarily the direction that the UAV is moving. Wind will introduce a crab angle χ_c that together with the heading ψ gives the course angle χ:

$$\chi = \psi + \chi_c. \tag{2.7}$$

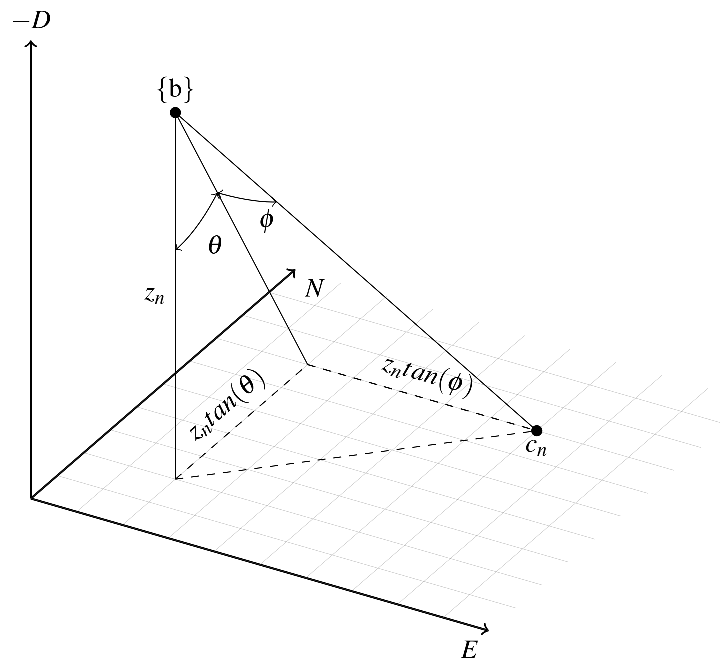

Figure 2.1: Illustration of how the aircraft attitude influence the camera position.

2.1.3 Camera Footprint

The camera footprint is coupled with all of the three angles given in $\boldsymbol{\Theta}$. The position of the camera footprint will be calculated using forward kinematics, and the situation is shown in figure 2.1.

Centre Position

The attitude of the UAV is given in the body frame $\{b\}$ and the height z_n is given in the NED frame $\{n\}$, and the model assumes flat earth. The position of the footprint centre point $\mathbf{c}_b^b$ in the body frame $\{b\}$ is expressed as the geometric (???) distance from the UAV position to the footprint centre point:

$$\mathbf{c}_b^b = \begin{bmatrix} c_{x/b}^b \\ c_{y/b}^b \end{bmatrix} = \begin{bmatrix} z_n tan(\theta) \\ z_n tan(\phi) \end{bmatrix}. \tag{2.8}$$

The coordinates of the camera position in $\{n\}$ can be found by rotating the point $\mathbf{c}_b^b$ with respect to the aircraft heading ψ, and by translating the rotated point to the aircrafts position in the $\{n\}$ frame. The rotation matrix for rotating with respect to the heading is given as

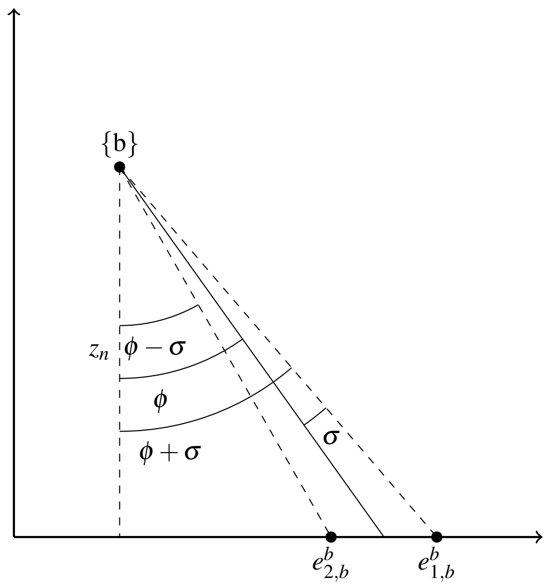

Figure 2.2: Illustration of how the field of view for a pushbroom sensor is calculated.

$$\mathbf{R}_{z,\psi} = \begin{bmatrix} cos(\psi) & -sin(\psi) \\ sin(\psi) & cos(\psi) \end{bmatrix}. \tag{2.9}$$

The final expression for the camera footprint centre position $\mathbf{c}^n$ in the $\{n\}$ frame then becomes:

$$\begin{aligned} \mathbf{c}^n &= \mathbf{p} + \mathbf{R}_{z,\psi}\mathbf{c}^b_b \\ &= \begin{bmatrix} x_n \\ y_n \end{bmatrix} + \mathbf{R}_{z,\psi} \begin{bmatrix} x^b_{x/b} \\ c^b_{y/b} \end{bmatrix} \end{aligned} \tag{2.10}$$

Edge Points

A hyperspectral pushbroom sensor captures images in a line, and the centre point of the camera footprint does not express the entire area that is captured by the sensor. The edge points of the camera footprint are calculated with respect to the sensor's field of view, as shown in figure 2.2. These points $\mathbf{e}$ can be found by altering 2.8:

$$\mathbf{e}^b_{1,b} = \begin{bmatrix} z_n tan(\theta) \\ z_n tan(\phi+\sigma) \end{bmatrix}, \ \mathbf{e}^b_{2,b} = \begin{bmatrix} z_n tan(\theta) \\ z_n tan(\phi-\sigma) \end{bmatrix}. \tag{2.11}$$

The steps for writing the edge points $\mathbf{e}$ in the $\{n\}$ is similar as in equation 2.10:

$$\mathbf{e}^n = \mathbf{p} + \mathbf{R}_{z,\psi}\mathbf{e}_b^b. \tag{2.12}$$

2.2 Optimization

In this chapter the methods and equations used for the optimization problem will be given. The goal of the optimization problem is to minimize the distance between the centre of the camera footprint and the path that is to be observed. The optimization problem will be given as an offline Model Predictive Control (MPC) problem, that includes the entire UAV model as constraints.

2.2.1 MPC Method

Model Predictive Control (MPC) is a control method that uses knowledge about the process to calculate the control signals. By calculating the future states of the process over a prediction horizon it calculates the control signals that will cause the process to follow a reference trajectory in the best way possible. The MPC strategy can be broken down into three tasks [14]:

1. Predict the future outputs of the process for the given prediction horizon using past inputs to the process and the past measured states of the process, and by using the future control signals.
2. Optimize an objective function in order to determine the future control signals that follows a given reference trajectory as closely as possible.
3. Apply the optimal control signals to the process, and measure the resulting output so that it may be used to calculate the next prediction horizon in the first task.

In short MPC problems are made up of three elements [14]: Prediction model, objective function and the control law. The prediction model represents the model of the process that is to be controlled, and will in this case consist of the differential equations for the states of the UAV. The objective function is the function that is to be minimized by the optimization algorithm, in this case this will be the distance from the camera centre point to the desired ground path together with some of the UAV states that will give a stable flight. The objective function represents the reference trajectory that the UAV is to follow. The control law introduces constraints on the problem, reducing the number of feasible solutions. This constraints can be put on either the states or the control inputs for the UAV.

A mathematical formulation of the three elements that make up the optimization problem is shown in 2.13 [15]. $f(x)$ represents the objective function that is subject to equality and inequality constraints respectively. The equality constraints are used to represent the UAV model, while the inequality constraints represent the constraints used for the control law. The control law may also consist of equality constraints.

$$\begin{aligned} \min_{x \in R^n} \quad & f(x) \\ \text{s.t} \quad & c_i(x) = 0, i \in \varepsilon, \\ & c_i(x) \geq 0, i \in I. \end{aligned} \tag{2.13}$$

2.2.2 Least-Squares Problem

$$f(x) = \frac{1}{2} \sum_{j=1}^{m} r_j^2(x) \tag{2.14}$$

In many applications the objective functions is formulated as a least-square (LSQ) problem and the general form of an LSQ is shown in equation 2.14 [15] where r_j is referred to as the residual function, and it is the function that we seek to minimize. This method is often used when problem involves measurements that is expected to follow a model that is known in advance. By formulating this as a LSQ problem and minmizing the resulting optimization problem, it is possible to find parameters that minimizes the difference between the model and the measurements.

The matching of measurements and a model relates to this task because the optimization problem will be given a path, and needs to find the best control inputs in order for the camera centre point to stay as close to this path as possible. However, since the path is prametrized and the position of the UAV on the path is not related to the path by time, there might be errors in calculating the difference between the path and the UAV. This is because the line between the UAV position and the closest parametrized point may not be orthogonal to the path.

To solve this problem orthogonal distance regression may be used [15]. This method adds a perturbation to one of the coordinates on the path and a perturbation to the UAV position. By minimizing these perturbations, the shortest distance from the path that is also orthogonal to the path can be found. How this relates to equation 2.14 is shown in equation 2.15a where δ is the added perturbation and d is the weighting of the perturbation. A visual representation is shown in figure **??**. The equations for the distance between the camera centre point and the path that it is to follow will be derived in the next subsection.

$$\min_{x,\delta} F(x,\delta) = \frac{1}{2} \sum_{j=1}^{2m} r_j^2(x,\delta) \tag{2.15a}$$

$$r_j(x,\delta) = \begin{cases} w_j[\phi(x;t_j+\delta_j) - y_j], & j = 1,2,...,m \\ d_{j-m}\delta_{j-m}, & j = m+1,...,2m \end{cases} \tag{2.15b}$$

2.2.3 Problem Definition

For the problem definition the 12 DOF UAV model presented by Beard & McLain [13] will be implemented. This means that the optimization vector will consist of 12 states, and there will be 4 control signals:

$$\mathbf{x} = \begin{bmatrix} p_N \\ p_E \\ p_D \\ u \\ v \\ w \\ \phi \\ \theta \\ \psi \\ p \\ q \\ r \end{bmatrix}, \quad \mathbf{u} = \begin{bmatrix} \delta_e \\ \delta_a \\ \delta_r \\ \delta_t \end{bmatrix}. \tag{2.16}$$

Prediction Model

The prediction model relates to the equality constraints of equation 2.13 in the form of differential equations. Based on the control inputs and current states, $\dot{\mathbf{x}}$ is calculated by the differential equation. The attitude angles will be expressed in Euler angles. Even though quaternions offer more efficient computations and no gimbal lock [13], this optimization will be run on an offboard computer/offline so that computation capacity is not a big issue and the UAV is not going to undergo any extreme maneuvers so that a gimbal lock should never occur.

Objective Function

The parametrized path that the camera is to observe will be given as a function $P(k)$ where k is the path paramter, and P is a $2xn$ matrix where the elements represent the position in p_E and p_N

$$\mathbf{P}(k) = \begin{bmatrix} \mathbf{p}_E(k) \\ \mathbf{p}_N(k) \end{bmatrix} = \begin{bmatrix} x_0 & x_1 & x_2 & \dots & x_n \\ y_0 & y_1 & y_2 & \dots & y_n \end{bmatrix}. \tag{2.17}$$

The residual function r will be defined as the difference between the observation path and the camera centre point $\mathbf{c}^n$ from equation 2.10:

$$r_j(x) = ||\mathbf{P}(k) - \mathbf{c}^n(x)||. \tag{2.18}$$

Control Law

The only physical constraints in this optimization problem is constraints on the control inputs, as shown in equation 2.19. This inequality constraint ensures that the control surfaces of the UAV simulated in the optimization do not excede what the UAV is physically capable of.

$$\mathbf{u}^{low} \leq \mathbf{u} \leq \mathbf{u}^{high} \tag{2.19}$$

Chapter 3

Optimization Implementation

3.1 ACADO toolkit

Chapter 4

System Overview

Appendices

Appendix A

UAV model

Bibliography

[1] E. Skjong, S. A. Nundal, F. S. Leira, and T. A. Johansen. 2015 international conference on unmanned aircraft systems (ICUAS). In *Autonomous Search and Tracking of Objects Using Model Predictive Control of Unmanned Aerial Vehicle and Gimbal: Hardware-in-the-loop Simulation of Payload and Avionics*, Denver, Colorado, USA, June 2015. IEEE.

[2] J. Egbert and R. W. Beard. Proceedings of the 2007 American control conference. In *Low Altitude Road Following Constraints Using Strap-Down EO Cameras on Miniature Air Vehicles*, New York City, USA, July 2007. IEEE.

[3] Thomas M. Fisher. Rudder augmented trajectory correction for unmanned aerial vehicles to decrease lateral image errors of fixed camera payloads. *All Graduate Theses and Dissertations*, 2016.

[4] S. Mills, J. J. Ford, and L. Mejias. Vision based control for fixed wing UAVs inspecting locally linear infrastructure using skid-to-turn maneuvers. *Journal of Intelligent and Robotic Systems*, 61(1):29–42, 2011.

[5] M. Ahsan, H. Rafique, and Z. Abbas. Multitopic conference (INMIC). In *Heading Control of a Fixed Wing UAV Using Alternate Control Surfaces*. IEEE, December 2012.

[6] T. Inanc, K. Misovec, and R. M. Murray. 43rd IEEE conference on decision and control. In *Nonlinear Trajectory Generation for Unmanned Air Vehicles with Multiple Radars*, Atlantis, Paradise Island, Bhamas, December 2004. IEEE.

[7] Anders la Cour-Harbo and Morten Bisgaard. *State-Control Trajectory Generation for Helicopter Slung Load System using Optimal Control*. American Institute of Aeronautics and Astronautics Meeting Papers on Disc. 2009.

[8] Stephen P. Jackson. Controlling small fixed wing UAVs to optimize image quality from on-board cameras. *ProQuest Dissertations and Theses*, 2011.

[9] Randall B. Smith. *Introduction to Hyperspectral Imaging*. MicroImages, Inc., 2012.

[10] R. Nsi, E. Honkavaara, P. Lyytikinen-Saarenmaa, M. Blomqvist, P. Litkey, T. Hakala, N. Viljanen, T. Kantola, T. Tanhuanp, and M. Holopainen. Using

UAV-based photogrammetry and hyperspectral imaging for mapping bark beetle damage at tree-level. *Remote Sensing*, 7(15467-15493), 2015.

[11] P. J. Zarco-Tejada, V. Gonzlez-Dugo, and J. A. J. Berni. Fluorescence, temperature and narrow-band indices acquired from a UAV platform for water stress detection using a micro-hyperspectral imager and a thermal camera. *Remote Sensing of Environment*, 117(322-337), 2012.

[12] J. Suomalainen, N. Anders, S. Iqbal, G. Roerink, J. Franke, P. Wenting, D. Hnniger, H. Bartholomeus, R. Becker, and L. Kooistra. A lightweight hyperspectral mapping system and photogrammetric processing chain for unmanned aerial vehicles. *Remote Sensing*, 6(11013-11030), 2014.

[13] Randal W. Beard and Timothy W. McLain. *Small Unmanned Aircraft: Theory and Practice*. Princeton University Press, Princeton, NJ, USA, 2012.

[14] E. F. Camacho and Bordons C. *Model Predictive Control*. Springer London, 1999.

[15] J. Nocedal and S. Wright. *Numerical Optimization*. Springer Series in Operations Research and Financial Engineering. Springer New York, 2006.